

Supporting Information

An ultrastable Zr-MOF for fast capture and highly luminescent detection of Cr₂O₇²⁻ simultaneously in aqueous phase

Xiaodong Sun,^a Shuo Yao,^a Chengyang Yu,^a Guanghua Li,^a Chunming Liu,*^b Qisheng Huo,^a and Yunling Liu*^a

^a State Key Laboratory of Inorganic Synthesis and Preparative Chemistry, College of Chemistry, Jilin University, Changchun 130012, P. R. China

E-mail: yunling@jlu.edu.cn; Fax: +86-431-85168624; Tel: +86-431-85168614

^b Central Laboratory, Changchun Normal University, 677 North Changji Road, Erdao District, Changchun 130032, China

E-mail: ccsf777@163.com

S1. Calculation procedures of selectivity from IAST

The measured experimental data is excess loadings (q^{ex}) of the pure components CO₂, CH₄, C₂H₆ and C₃H₈ for **JLU-MOF50**, which should be converted to absolute loadings (q) firstly.

$$q = q^{ex} + \frac{pV_{pore}}{ZRT}$$

Here Z is the compressibility factor. The Peng-Robinson equation was used to estimate the value of compressibility factor to obtain the absolute loading, while the measure pore volume 0.53 cm³ g⁻¹ is also necessary.

The dual-site Langmuir-Freundlich equation is used for fitting the isotherm data at 298 K.

$$q = q_{m1} \times \frac{b_1 \times p^{1/n_1}}{1 + b_1 \times p^{1/n_1}} + q_{m2} \times \frac{b_2 \times p^{1/n_2}}{1 + b_2 \times p^{1/n_2}}$$

Here p is the pressure of the bulk gas at equilibrium with the adsorbed phase (kPa), q is the adsorbed amount per mass of adsorbent (mol kg⁻¹), q_{m1} and q_{m2} are the saturation capacities of sites 1 and 2 (mol kg⁻¹), b_1 and b_2 are the affinity coefficients of sites 1 and 2 (1/kPa), n_1 and n_2 are the deviations from an ideal homogeneous surface.

The selectivity of preferential adsorption of component 1 over component 2 in a mixture containing 1 and 2, perhaps in the presence of other components too, can be formally defined as

$$S = \frac{q_1/q_2}{p_1/p_2}$$

q_1 and q_2 are the absolute component loadings of the adsorbed phase in the mixture. These component loadings are also termed the uptake capacities. We calculate the values of q_1 and q_2 using the Ideal

Adsorbed Solution Theory (IAST) of Myers and Prausnitz.

S2. Supporting Figures

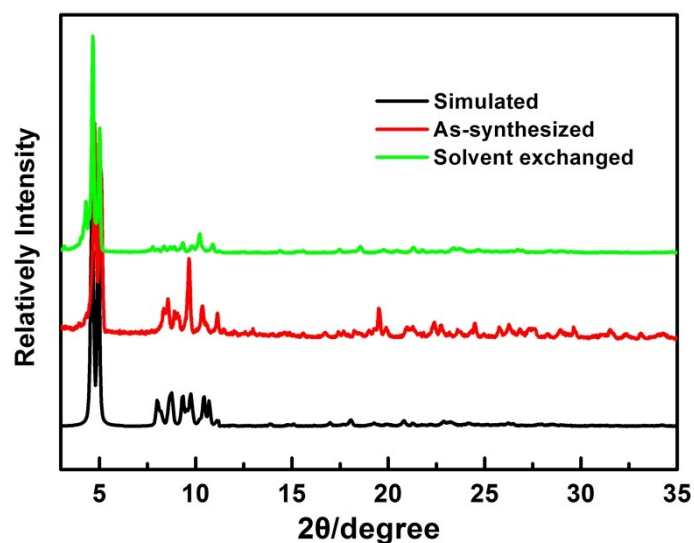


Fig. S1 PXRD patterns of **JLU-MOF50** for simulated, as-synthesized and CH₃CN solvent exchanged samples.

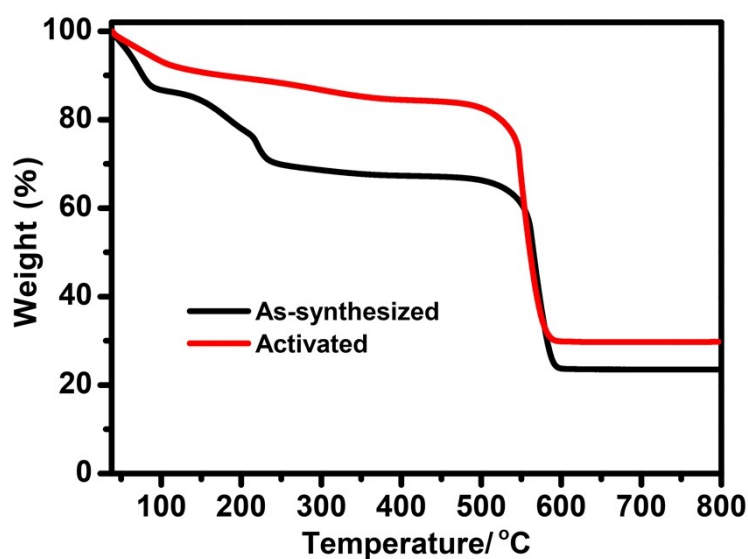


Fig. S2 TGA curves of **JLU-MOF50** for the as-synthesized and activated samples.

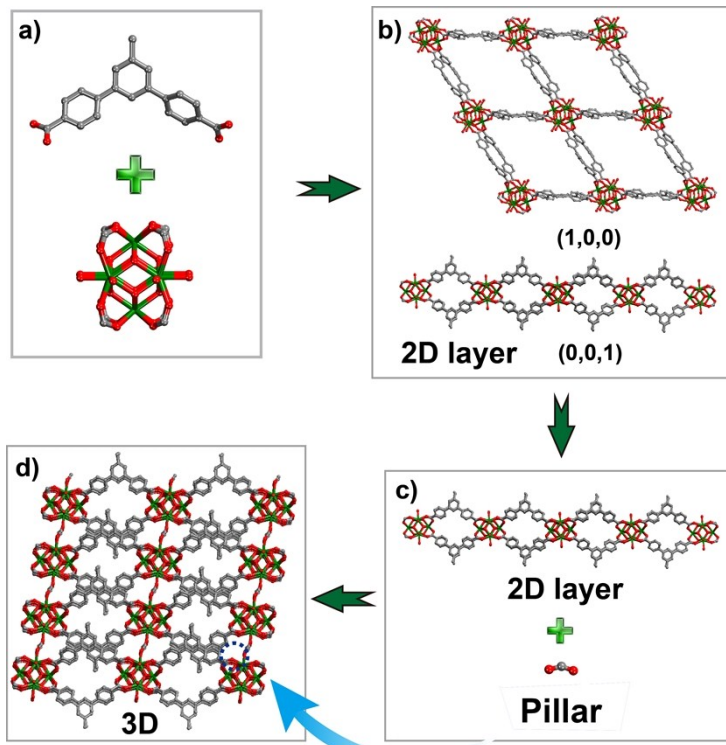


Fig. S3 The formation process of **JLU-MOF50**. The Zr₆ clusters are weaved by V-shaped ligands (a) to configure a 2D layer which can be seen from (1, 0, 0) and (0, 0, 1) directions (b). The 2D layer further pillared by formic acid to fabricate the 3D framework (c and d). (Color scheme: carbon = grey; oxygen = red; zirconium = dark green).

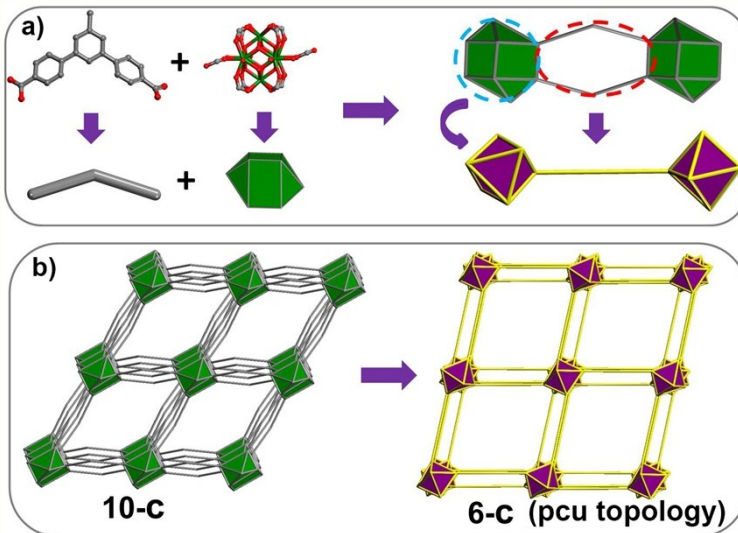


Fig. S4 (a) Double walled building blocks were assembled by two 10-connected Zr₆ SBUs with distorted dodecahedron geometry and two C₂-symmetric H₂MDCPB ligands with V-shaped rod. Due to the presence of double walls, the distorted dodecahedron can be simplified as octahedron, and the double walls can be simplified as linear rod. (b) The 10-c building blocks with double wall can be simplified to a 6-c node with **pcu** topology.

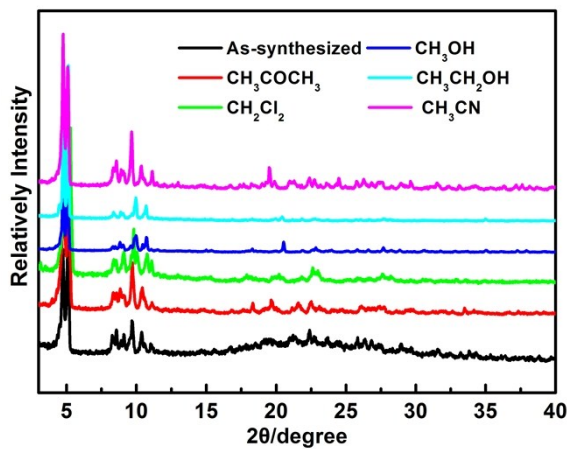


Fig. S5 PXRD patterns of **JLU-MOF50** samples for as-synthesized and immersed in different organic solutions at room temperature for 48 h, which indicate the stability of the framework in different organic solutions.

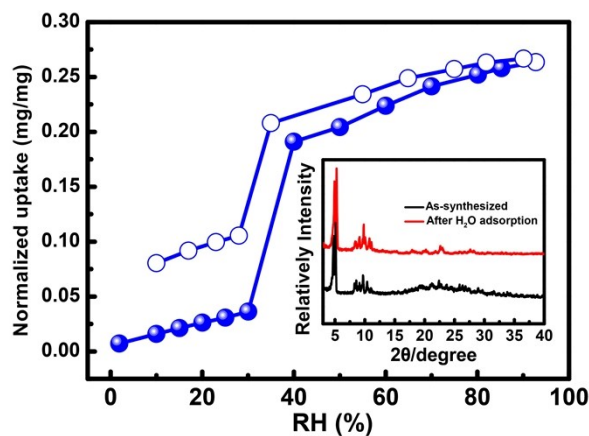


Fig. S6 Water adsorption isotherm of **JLU-MOF50** (experimental condition: $T = 298 \text{ K}$, $P = 1 \text{ bar}$; N_2 carrier gas). PXRD patterns (insert graph) for **JLU-MOF50** sample before and after measuring the water adsorption isotherm, which indicate the water stability of the framework.

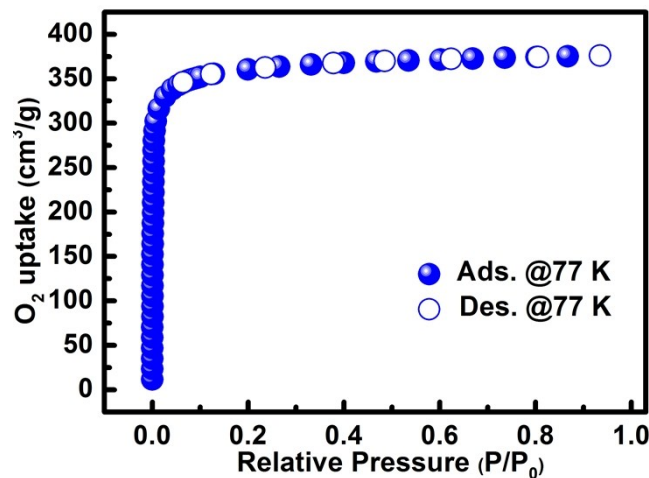


Fig. S7 The O_2 adsorption isotherm for **JLU-MOF50** at 77 K under 1 bar.

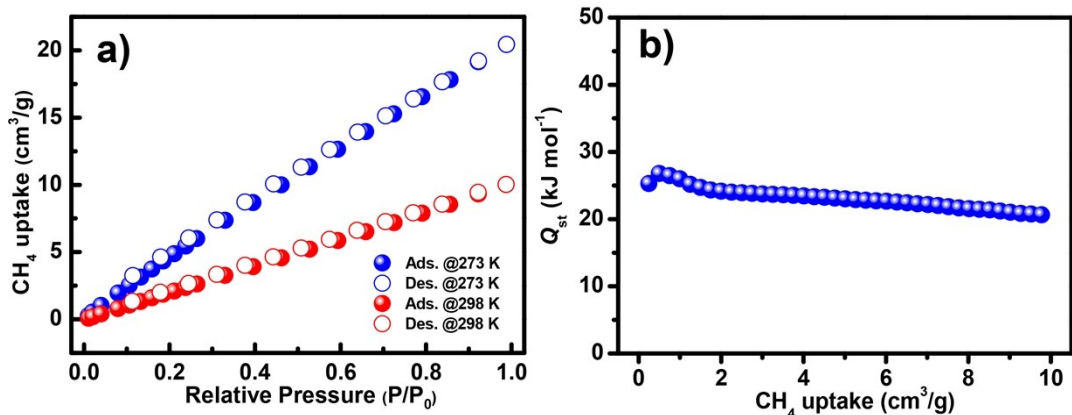


Fig. S8 The CH₄ adsorption isotherms for **JLU-MOF50** at 273 and 298 K under 1 bar and Q_{st} of CH₄ for **JLU-MOF50**.

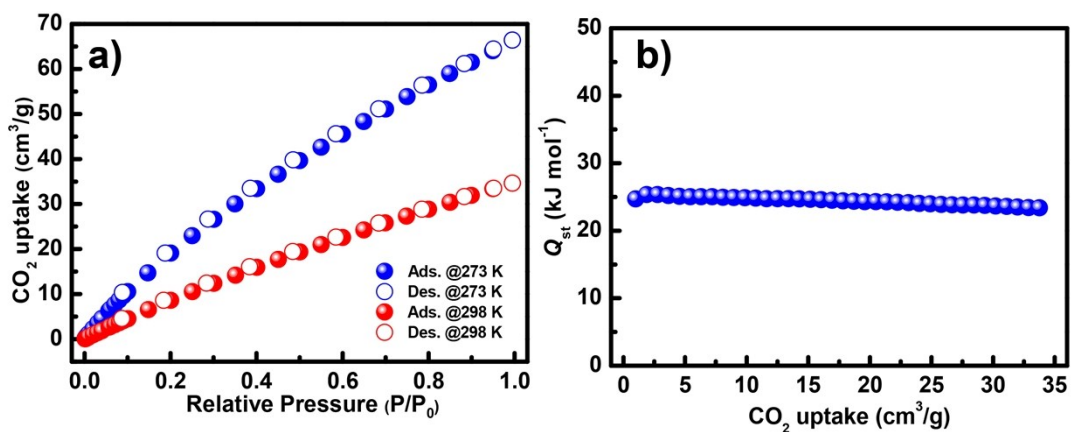


Fig. S9 The CO₂ adsorption isotherms for **JLU-MOF50** at 273 and 298 K under 1 bar and Q_{st} of CO₂ for **JLU-MOF50**.

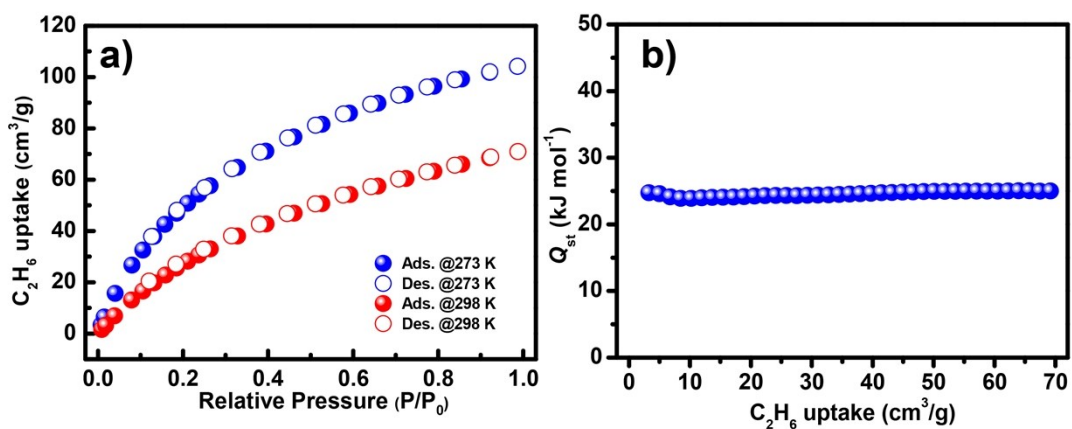


Fig. S10 The C₂H₆ adsorption isotherms for **JLU-MOF50** at 273 and 298 K under 1 bar and Q_{st} of C₂H₆ for **JLU-MOF50**.

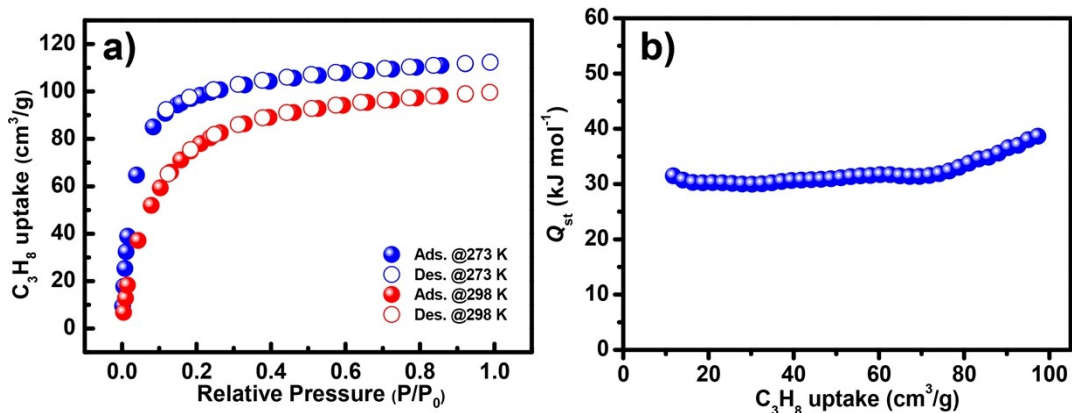


Fig. S11 The C_3H_8 adsorption isotherms for **JLU-MOF50** at 273 and 298 K under 1 bar and Q_{st} of C_3H_8 for **JLU-MOF50**.

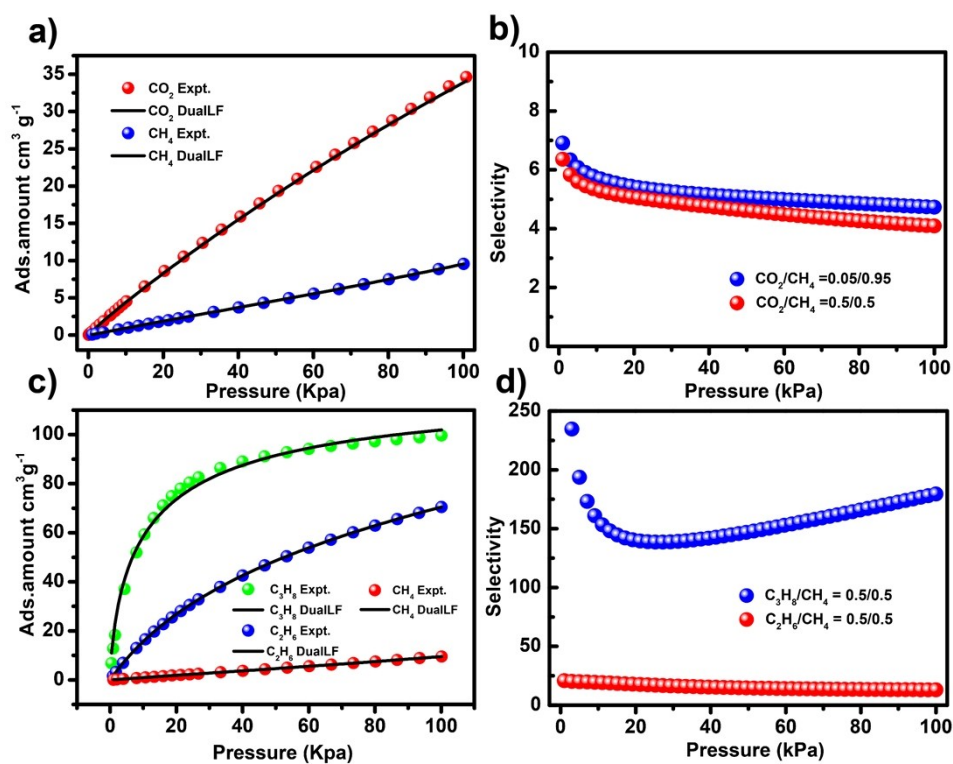


Fig. S12 CO_2 , CH_4 , C_2H_6 and C_3H_8 adsorption isotherms at 298 K along with the dual-site Langmuir-Freudlich (DSLF) fits (a and c); gas mixture adsorption selectivity are predicted by IAST at 298 K and 100 kPa for **JLU-MOF50** (b and d).

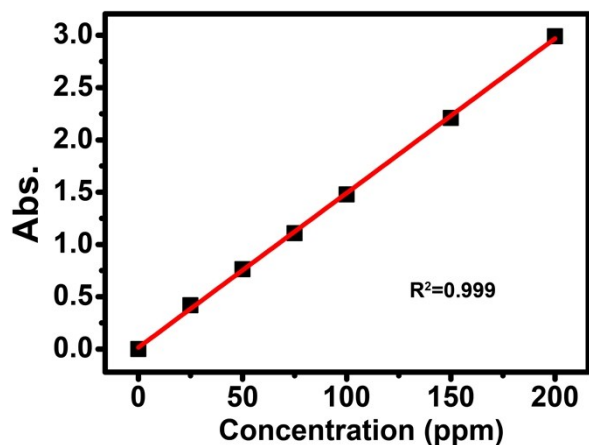


Fig. S13 The standard curve line of $\text{Cr}_2\text{O}_7^{2-}$ was performed and the concentration of $\text{Cr}_2\text{O}_7^{2-}$ has a good linear relationship with its absorbance ($R^2 > 0.999$). The fitting parameter was then to predict the remaining $\text{Cr}_2\text{O}_7^{2-}$ in aqueous phase after adsorption.

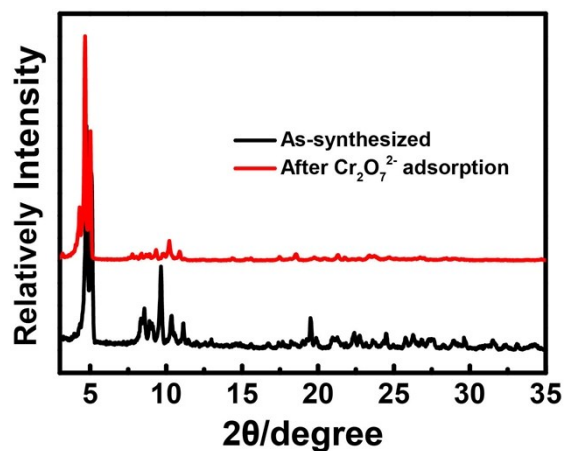


Fig. S14 PXRD patterns for **JLU-MOF50** samples before and after measuring the $\text{Cr}_2\text{O}_7^{2-}$ adsorption which indicate the stability of the framework.

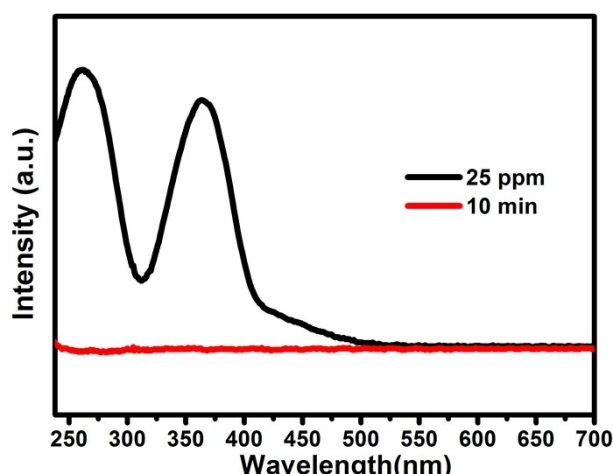


Fig. S15 UV-vis spectra for the $\text{Cr}_2\text{O}_7^{2-}$ adsorption behavior of **JLU-MOF50** at low concentration (25 ppm).

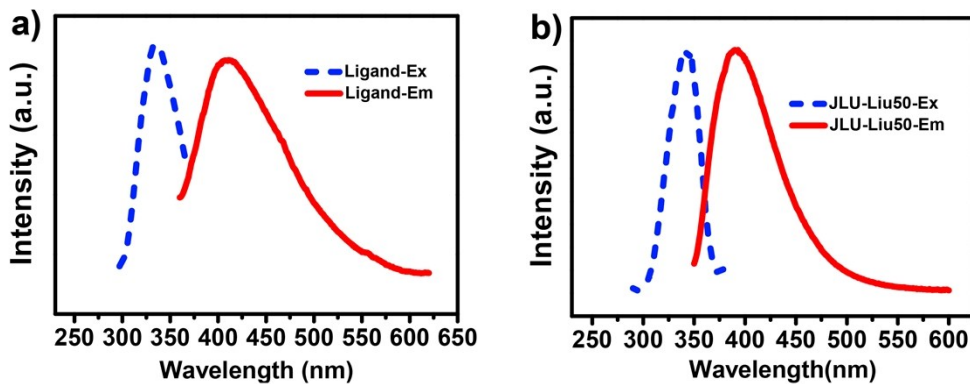


Fig. S16 The solid-state excitation (dot lines) and emission (solid lines) spectra of free H₂MDCPB ligand (a) and **JLU-MOF50** (b). The free H₂MDCPB ligand exhibits fluorescent emissions at 411 nm upon excitation at 340 nm. Compared with the free ligand, **JLU-MOF50** exhibits a similar emission at 397 nm under the same excitation

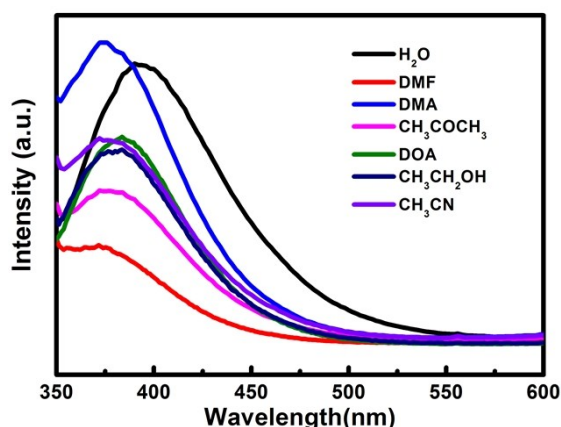


Fig. S17 Effect on the emission spectra of **JLU-MOF50** dispersed in different solvents: water, DMF, DMA, acetone, dioxane, ethanol and acetonitrile. It was found that the fluorescent emissions have a little solvent dependence. A certain degree of fluorescent quenching was observed in DMF and acetone solvents, and **JLU-MOF50** exhibits excellent fluorescence intensity in water and DMA solvents. Considering the practicality of the material, we select water as the solvent.

The quenching efficiency was calculated by using the Stern-Volmer (SV) equation ($I_0/I = K_{SV}[Q] + 1$, where I_0 and I are the fluorescence intensities before and after the addition of the analytes, Q is the molar concentration of the analytes and K_{SV} is the quenching constant (M^{-1})). The K_{SV} values can be evaluated accurately when the $(I_0/I)/[Q]$ plot is linear.

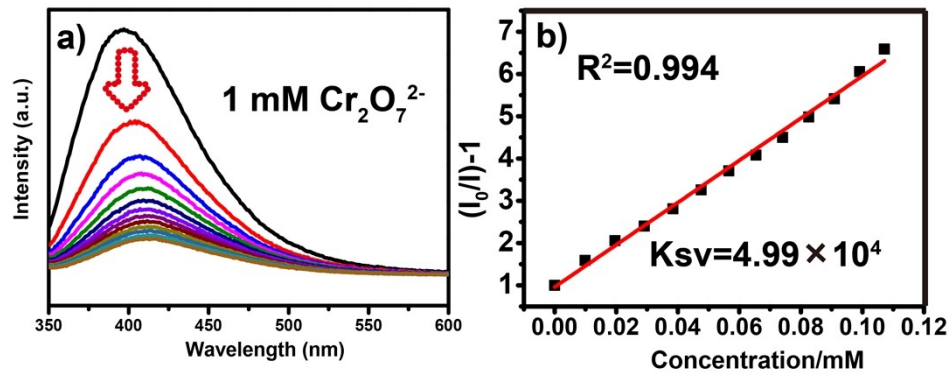


Fig. S18 a) Effect on the emission spectra of **JLU-MOF50** dispersed in water upon the incremental addition of 240 μ L (1 mM, 20 μ L addition each time) aqueous solution of $\text{Cr}_2\text{O}_7^{2-}$. b) SV plot of $\text{Cr}_2\text{O}_7^{2-}$.

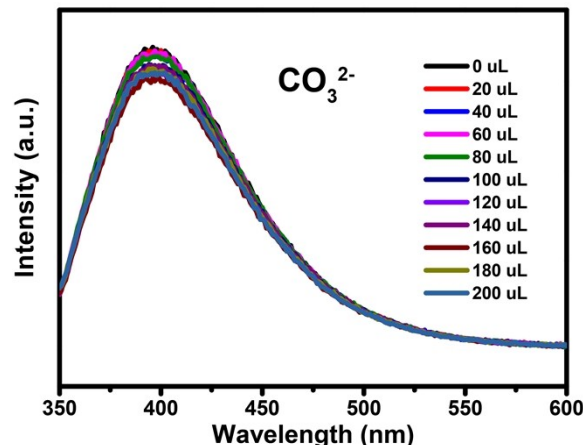


Fig. S19 Effect on the emission spectra of **JLU-MOF50** dispersed in water upon the incremental addition of 200 μ L (10 mM, 20 μ L addition each time) aqueous solution of CO_3^{2-} .

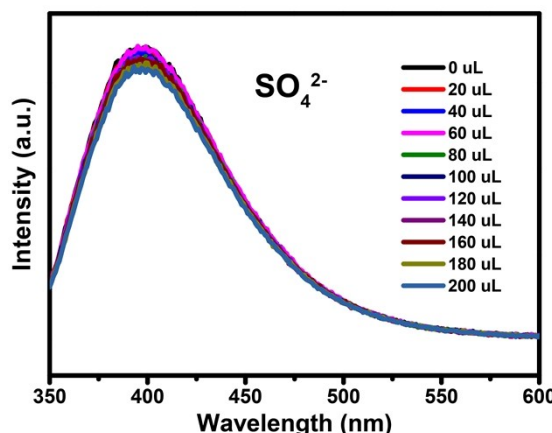


Fig. S20 Effect on the emission spectra of **JLU-MOF50** dispersed in water upon the incremental addition of 200 μ L (10 mM, 20 μ L addition each time) aqueous solution of SO_4^{2-} .

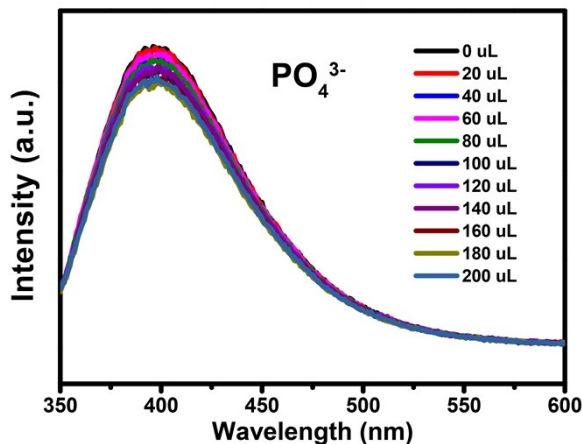


Fig. S21 a) Effect on the emission spectra of **JLU-MOF50** dispersed in water upon the incremental addition of 200 μL (10 mM, 20 μL addition each time) aqueous solution of PO_4^{3-} .

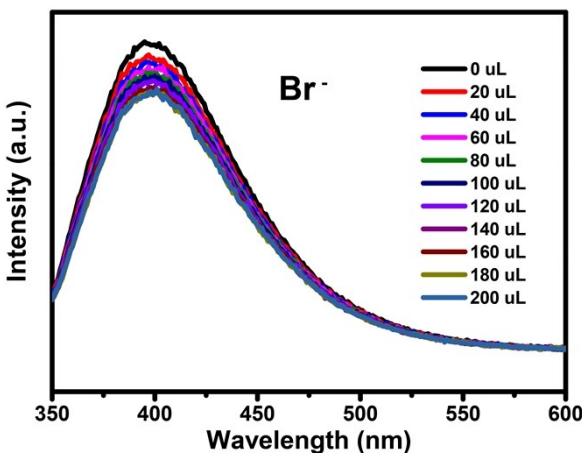


Fig. S22 a) Effect on the emission spectra of **JLU-MOF50** dispersed in water upon the incremental addition of 200 μL (10 mM, 20 μL addition each time) aqueous solution of Br^- .

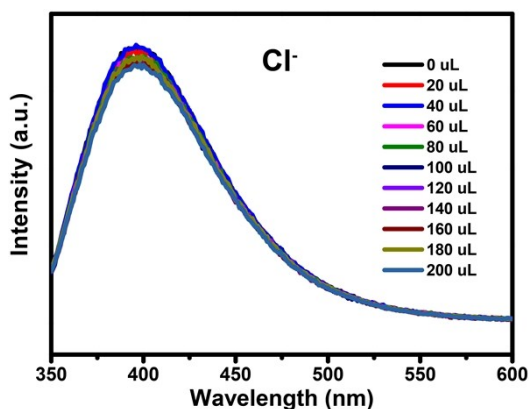


Fig. S23 a) Effect on the emission spectra of **JLU-MOF50** dispersed in water upon the incremental addition of 200 μL (10 mM, 20 μL addition each time) aqueous solution of Cl^- .

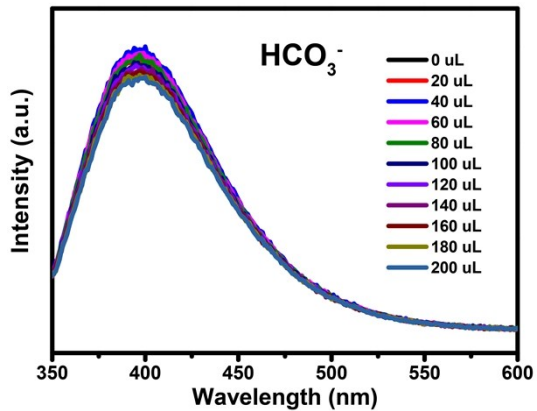


Fig. S24 a) Effect on the emission spectra of **JLU-MOF50** dispersed in water upon the incremental addition of 200 μL (10 mM, 20 μL addition each time) aqueous solution of HCO_3^- .

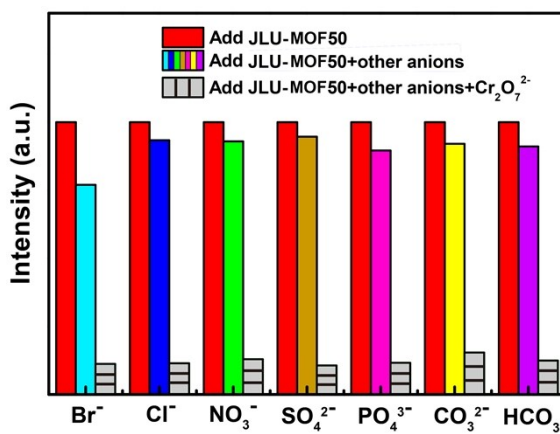


Fig. S25 The selective detection of $\text{Cr}_2\text{O}_7^{2-}$ on **JLU-MOF50** in the presence of other anions in the water (red bars: Fluorescence intensity of **JLU-MOF50** dispersed in the water; multicolor bars: Fluorescence intensity of **JLU-MOF50** dispersed in the water with the addition of 100 μL 10 mM different anions; grey bars: Fluorescence intensity of **JLU-MOF50** dispersed in the water with the addition of 100 μL 10 mM different anions and 20 μL 10 mM $\text{Cr}_2\text{O}_7^{2-}$ solution).

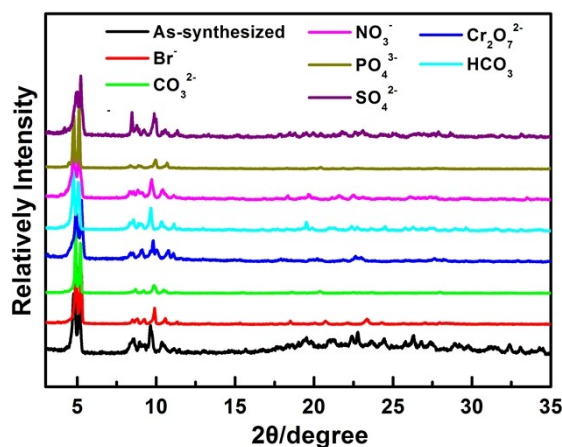


Fig. S26 PXRD patterns of **JLU-MOF50** after the detection of different kinds of anions, which indicates the stability of the framework.

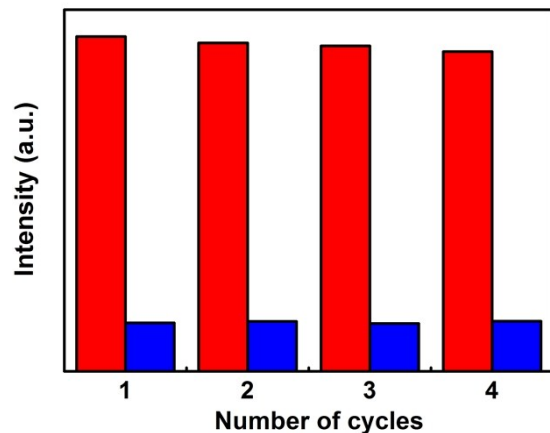


Fig. S27 Reproducibility of the quenching ability of **JLU-MOF50** dispersed in water in the presence of 240 μL 1mM aqueous solution of $\text{Cr}_2\text{O}_7^{2-}$.

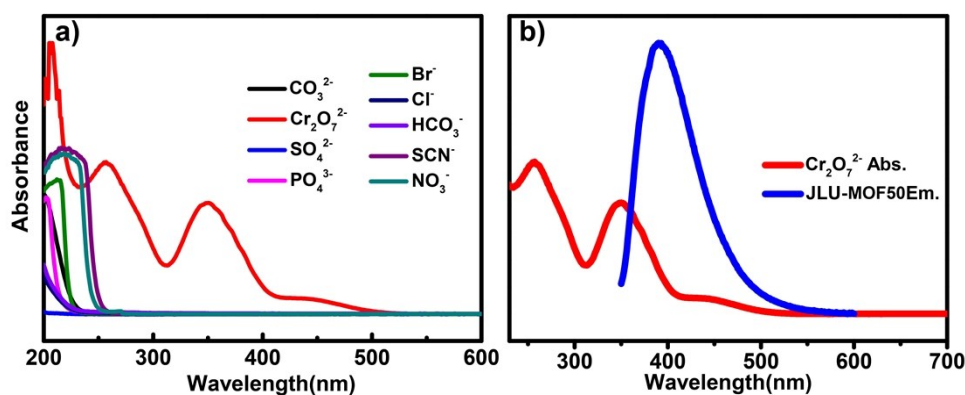


Fig. S28 (a) UV-vis spectra of different anions in aqueous solutions; (b) the overlap between the emission spectrum of the **JLU-MOF50** and the absorption spectrum of the $\text{Cr}_2\text{O}_7^{2-}$.

S3. Supporting Tables

Table S1. A comparison of chemical stability of **JLU-MOF50** with other stable Zr-MOFs materials

Compound	pH values	Reference
JLU-MOF50	0-11	This work
PCN-223	0-10	1
PCN-777	3-11	2
PCN-56	2-11	3
PCN-59	2-11	3
PCN-225	0-12	4
BUT-12	0-10	5
BUT-13	0-10	5
BUT-14	0-10	6
BUT-15	0-10	6
NPF-200	1-12	7
PCN-134	0-13	8

Table S2. Crystal data and structure refinement for **JLU-MOF50**

formula	C ₁₁₅ H ₁₅₅ N ₉ O ₅₃ Zr ₆
formula weight	3058.80
temp (K)	293(2) K
wavelength (Å)	0.71073 Å
crystal system, space group	Triclinic, P-1
a (Å)	10.624(2)
b (Å)	19.309(4)
c (Å)	19.483(4)
V (Å ³)	3493.7(12)
Z, D _c (Mg/m ³)	1, 1.454
F(000)	1572
θ range (deg)	1.18 to 25.78°
reflns collected/unique	23440/13036
R _{int}	0.0499
data/restraints/params	13036/50/586
GOF on F ²	0.980
R ₁ , wR ₂ (I>2σ(I))	R ₁ = 0.0506, wR ₂ = 0.1370
R ₁ , wR ₂ (all data)	R ₁ = 0.0688, wR ₂ = 0.1455

Table S3. Selected bond lengths [Å] and angles [°] for **JLU-MOF50**.

Zr(1)-O(5)	2.164(3)	O(5)-C(34)	1.279(5)
Zr(1)-O(10)	2.165(4)	O(6)-C(34)	1.251(5)
Zr(1)-O(11)	2.171(4)	O(7)-C(41)	1.238(6)
Zr(1)-O(12)	2.183(4)	O(8)-C(41)	1.259(6)
Zr(1)-O(1)	2.187(3)	O(13)-C(43)	1.381(16)
Zr(1)-O(9)	2.201(4)	O(15)-C(44)	1.137(11)
Zr(2)-O(10)	2.128(4)	C(1)-C(2)	1.381(6)
Zr(2)-O(9)	2.131(4)	C(1)-C(6)	1.396(7)
Zr(2)-O(15)	2.174(3)	C(1)-C(7)	1.482(7)
Zr(2)-O(14)	2.213(5)	C(2)-C(3)	1.380(6)
Zr(2)-O(2)	2.261(3)	C(3)-C(4)	1.389(7)
Zr(3)-O(11)	2.133(3)	C(3)-C(14)	1.490(6)
Zr(3)-O(9)	2.137(4)	C(2)-C(1)-C(6)	116.8(4)
Zr(3)-O(13)	2.158(3)	C(2)-C(1)-C(7)	119.9(4)
Zr(3)-O(16)	2.214(4)	C(6)-C(1)-C(7)	123.2(4)
O(1)-C(13)	1.252(6)	C(3)-C(2)-C(1)	122.1(5)
O(2)-C(13)	1.261(5)	C(4)-C(5)-C(6)	119.0(5)
O(3)-C(20)	1.255(5)	C(4)-C(5)-C(21)	119.7(5)
O(4)-C(20)	1.263(5)	C(6)-C(5)-C(21)	121.3(4)

Symmetry transformations used to generate equivalent atoms:

#1 -x,-y+2,-z+1 #2 -x+1,-y+1,-z+1 #3 -x+1,-y+2,-z #4 x,y+1,z-1 #5 x+1,y,z-1
#6 x-1,y,z+1 #7 x,y-1,z+1 #8 -x+2,-y+2,-z

Table S4. Gas adsorption data for **JLU-MOF50**.

Gas	O ₂ (cm ³ g ⁻¹)		CO ₂ (cm ³ g ⁻¹)		CH ₄ (cm ³ g ⁻¹)	
	Temperature	77 K	273 K	298 K	273 K	298 K
Ads. amount		376	116	66	20	11
Gas	C ₂ H ₆ (cm ³ g ⁻¹)		C ₃ H ₈ (cm ³ g ⁻¹)		H ₂ O (mg/mg)	
Temperature	273 K	298 K	273 K	298 K	298 K	
Ads. amount	104	71	112	100	0.26 mg/mg	

Table S5. Comparison of detection ability of **JLU-MOF50** with fluorescent MOFs materials towards $\text{Cr}_2\text{O}_7^{2-}$.

MOFs materials	Responsive time	Quenching constant(M^{-1})	Recyclability	Solvent	Ref.
JLU-MOF50	seconds	4.99×10^4	Yes	water	This work
Zn-MOF-1	seconds	2.07×10^4	Yes	water	9
[Zn ₂ (TPOM)(NH ₂ -BDC) ₂]·4H ₂ O	seconds	7.59×10^3	Yes	DMF	10
[Zn ₂ (TPOM)(BDC) ₂]·4H ₂ O	seconds	4.45×10^3	Yes	DMF	10
[Cd(L)(TPOM)0.75].xS	seconds	1.35×10^4	Yes	water	11
[Zn(L)(BBI)·(H ₂ O) ₂]	seconds	1.17×10^4	Yes	water	11
[Zn(2-NH ₂ bdc)(bibp)] _n	seconds	—	No	water	12
[Eu(Hpzbc) ₂ (NO ₃)]<·H ₂ O	—	—	No	ethanol	13
[Zn ₂ (tpeb) ₂ (2,3-ndc) ₂]·H ₂ O] _n	seconds	—	Yes	water	14
[Zn ₂ (TPOM)(NDC) ₂]·3.5H ₂ O	seconds	9.21×10^3	—	water	15
[Cd(TPTZ)(H ₂ O) ₂ (HCOOH)	12 h	—	No	water	16
(IPA) ₂] _n					
534-MOF-Tb	seconds	1.37×10^4	Yes	water	17
Eu ³⁺ @MIL-121	24 h	4.34×10^3	No	water	18
[Zn ₇ (TPPE) ₂ (SO ₄ ²⁻) ₇](DMF·H ₂ O)	seconds	1.09×10^4	—	water	19
[Tb(TATAB)(H ₂ O) ₂]<·NMP	—	1.11×10^4	No	water	20
[Zn ₃ (tza) ₂ (μ ₂ -OH) ₂ (H ₂ O) ₂]H ₂ O	seconds	5.02×10^3	Yes	water	21
[Zn(btz)] _n	—	3.19×10^3	Yes	water	22
[Zn ₂ (ttz)H ₂ O] _n	—	2.19×10^3	Yes	water	22
[Eu(ipbp) ₂ (H ₂ O) ₃]Br ₆ H ₂ O	seconds	8.98×10^3	Yes	water	23

Table S6. Comparison of $\text{Cr}_2\text{O}_7^{2-}$ adsorption ability of **JLU-MOF50** with MOFs and other type adsorbents.

MOF based Adsorbents	Maximum Capacity (mg g^{-1})	Ref.
ZJU-101	245	24
ABT·2ClO ₄	214	25
Ag(L ²⁴³)]<·(CF ₃ CO ₂)(H ₂ O)	207	26
L-SO ₄	166	27
FIR-54	103	28
JLU-MOF50	92	This work
FIR-53	74	28
SLUG-35	68	29
1-ClO ₄	63	30
SLUG-21	60	31
PCN-134	57	32
MOF-867	53	24

Other Type Adsorbents	Maximum Capacity (mg g ⁻¹)	Ref.
Porous organic polymers	172	33
NH ₂ -TNTs	154	34
Ethylenediamine-functionalized Fe ₃ O ₄ magnetic polymers	61	35
β-CD and quaternary ammonium groups modified cellulose	61	36
Modified magnetic chitosan chelating	58	37
Saw dust	42	38
Eichhornia crassipes root biomass-derived activated carbon	36	39
Wheat-residue derived black carbon	21	40
Calcined LDHs	17	31
Hexadecylpyridinium bromide modified natural zeolites	14	41
Amino strach	12	42
uncalcined LDHs	6	41

REFERENCES

- D. Feng, Z. Y. Gu, Y. P. Chen, J. Park, Z. Wei, Y. Sun, M. Bosch, S. Yuan and H. C. Zhou, *J. Am. Chem. Soc.*, 2014, **136**, 17714-17717.
- D. Feng, K. Wang, J. Su, T. F. Liu, J. Park, Z. Wei, M. Bosch, A. Yakovenko, X. Zou and H. C. Zhou, *Angew. Chem. Int. Ed.*, 2015, **54**, 149-154.
- H. L. Jiang, D. Feng, T. F. Liu, J. R. Li and H. C. Zhou, *J. Am. Chem. Soc.*, 2012, **134**, 14690-14693.
- H. L. Jiang, D. Feng, K. Wang, Z. Y. Gu, Z. Wei, Y. P. Chen and H. C. Zhou, *J. Am. Chem. Soc.*, 2013, **135**, 13934-13938.
- B. Wang, X. L. Lv, D. Feng, L. H. Xie, J. Zhang, M. Li, Y. Xie, J. R. Li and H. C. Zhou, *J. Am. Chem. Soc.*, 2016, **138**, 6204-6216.
- B. Wang, Q. Yang, C. Guo, Y. Sun, L. H. Xie and J. R. Li, *ACS Appl. Mater. Interfaces*, 2017, **9**, 10286-10295.
- X. Zhang, X. Zhang, J. A. Johnson, Y. S. Chen and J. Zhang, *J. Am. Chem. Soc.*, 2016, **138**, 8380-8383.
- S. Yuan, J. S. Qin, L. Zou, Y. P. Chen, X. Wang, Q. Zhang and H. C. Zhou, *J. Am. Chem. Soc.*, 2016, **138**, 6636-6642.
- X.-Y. Guo, F. Zhao, J.-J. Liu, Z.-L. Liu and Y.-Q. Wang, *J. Mater. Chem. A*, 2017, **5**, 20035-20043.
- R. Lv, J. Wang, Y. Zhang, H. Li, L. Yang, S. Liao, W. Gu and X. Liu, *J. Mater. Chem. A*, 2016, **4**, 15494-15500.
- Y. Zhao, X. Xu, L. Qiu, X. Kang, L. Wen and B. Zhang, *ACS Appl. Mater. Interfaces*, 2017, **9**, 15164-15175.
- L. Wen, X. Zheng, K. Lv, C. Wang and X. Xu, *Inorg. Chem.*, 2015, **54**, 7133-7135.
- G.-P. Li, G. Liu, Y.-Z. Li, L. Hou, Y.-Y. Wang and Z. Zhu, *Inorg. Chem.*, 2016, **55**, 3952-3959.
- T.-Y. Gu, M. Dai, D. J. Young, Z.-G. Ren and J.-P. Lang, *Inorg. Chem.*, 2017, **56**, 4668-4678.
- R. Lv, H. Li, J. Su, X. Fu, B. Yang, W. Gu and X. Liu, *Inorg. Chem.*, 2017, **56**, 12348-12356.
- Y. Wang, L. Cheng, Z.-Y. Liu, X.-G. Wang, B. Ding, L. Yin, B.-B. Zhou, M.-S. Li, J.-X. Wang

- and X.-J. Zhao, *Chem.-Eur. J.*, 2015, **21**, 14171-14178.
- 17. M. Chen, W.-M. Xu, J.-Y. Tian, H. Cui, J.-X. Zhang, C.-S. Liu and M. Du, *J. Mater. Chem. C*, 2017, **5**, 2015-2021.
 - 18. J.-N. Hao and B. Yan, *New J. Chem.*, 2016, **40**, 4654-4661.
 - 19. X.-X. Wu, H.-R. Fu, M.-L. Han, Z. Zhou and L.-F. Ma, *Cryst. Growth Des.*, 2017, **17**, 6041-6048.
 - 20. G.-X. Wen, M.-L. Han, X.-Q. Wu, Y.-P. Wu, W.-W. Dong, J. Zhao, D.-S. Li and L.-F. Ma, *Dalton Trans.*, 2016, **45**, 15492-15499.
 - 21. T.-Q. Song, J. Dong, H.-L. Gao, J.-Z. Cui and B. Zhao, *Dalton Trans.*, 2017, **46**, 13862-13868.
 - 22. C.-S. Cao, H.-C. Hu, H. Xu, W.-Z. Qiao and B. Zhao, *CrystEngComm*, 2016, **18**, 4445-4451.
 - 23. C. Zhang, L. Sun, Y. Yan, H. Shi, B. Wang, Z. Liang and J. Li, *J. Mater. Chem. C*, 2017, **5**, 8999-9004.
 - 24. Q. Zhang, J. Yu, J. Cai, L. Zhang, Y. Cui, Y. Yang, B. Chen and G. Qian, *Chem. Commun.*, 2015, **51**, 14732-14734.
 - 25. X. Li, H. Xu, F. Kong and R. Wang, *Angew. Chem., Int. Ed.*, 2013, **52**, 13769-13773.
 - 26. C.-P. Li, H. Zhou, S. Wang, J. Chen, Z.-L. Wang and M. Du, *Chem. Commun.*, 2017, **53**, 9206-9209.
 - 27. A. V. Desai, B. Manna, A. Karmakar, A. Sahu and S. K. Ghosh, *Angew. Chem. Int. Ed.*, 2016, **55**, 7811-7815.
 - 28. H.-R. Fu, Z.-X. Xu and J. Zhang, *Chem. Mater.*, 2015, **27**, 205-210.
 - 29. H. Fei, C. S. Han, J. C. Robins and S. R. J. Oliver, *Chem. Mater.*, 2013, **25**, 647-652.
 - 30. P.-F. Shi, B. Zhao, G. Xiong, Y.-L. Hou and P. Cheng, *Chem. Commun.*, 2012, **48**, 8231-8233.
 - 31. H. Fei, M. R. Bresler and S. R. J. Oliver, *J. Am. Chem. Soc.*, 2011, **133**, 11110-11113.
 - 32. S. Yuan, J.-S. Qin, L. Zou, Y.-P. Chen, X. Wang, Q. Zhang and H.-C. Zhou, *J. Am. Chem. Soc.*, 2016, **138**, 6636-6642.
 - 33. Y. Su, Y. Wang, X. Li, X. Li and R. Wang, *ACS Appl. Mater. Interfaces*, 2016, **8**, 18904-18911.
 - 34. L. Wang, W. Liu, T. Wang and J. Ni, *Chem. Eng. J.*, 2013, **225**, 153-163.
 - 35. Y.-G. Zhao, H.-Y. Shen, S.-D. Pan and M.-Q. Hu, *J. Hazard. Mater.*, 2010, **182**, 295-302.
 - 36. Y. Zhou, Q. Jin, T. Zhu and Y. Akama, *J. Hazard. Mater.*, 2011, **187**, 303-310.
 - 37. Y. G. Abou El-Reash, M. Otto, I. M. Kenawy and A. M. Ouf, *Int. J. Biol. Macromol.*, 2011, **49**, 513-522.
 - 38. S. Gupta and B. V. Babu, *Chem. Eng. J.*, 2009, **150**, 352-365.
 - 39. A. K. Giri, R. Patel and S. Mandal, *Chem. Eng. J.*, 2012, **185**, 71-81.
 - 40. X. S. Wang, L. F. Chen, F. Y. Li, K. L. Chen, W. Y. Wan and Y. J. Tang, *J. Hazard. Mater.*, 2010, **175**, 816-822.
 - 41. Y. Zeng, H. Woo, G. Lee and J. Park, *Microporous Mesoporous Mater.*, 2010, **130**, 83-91.
 - 42. A. Dong, J. Xie, W. Wang, L. Yu, Q. Liu and Y. Yin, *J. Hazard. Mater.*, 2010, **181**, 448-454.